Supplemental Information

Additive manufacture of lightly crosslinked semicrystalline thiol-enes for enhanced mechanical performance

Kimberly K. Childress[1], Marvin D. Alim[2], Juan J. Hernandez[1], Jeffrey W. Stansbury[1,3], Christopher N. Bowman[1,2]

[1]Department of Chemical and Biological Engineering, University of Colorado Boulder, 3415 Colorado Avenue, Boulder, Colorado 80303, United States

[2]Materials Science and Engineering Program, University of Colorado Boulder, 596 UCB, Boulder, Colorado 80309, United States

[3]Department of Craniofacial Biology, School of Dental Medicine, University of Colorado Denver, 12800 East 19th Avenue, Aurora, Colorado 80045, United States

Table S1 Mechanical properties obtained for different crosslinkers at different concentrations. ASTM D638 Type V dogbones were cut from a bulk film approximately 500 μm thick (prepared between glass slides and irradiated with a 405 nm LED UV bar for 10 minutes on each side) and uniaxially strained at 5 mm min^{-1}.

|	E (MPa)	Yield Stress (MPa)	Ultimate Tensile Stress (MPa)	Elongation at break (%)	Toughness (MJ m^{-3})
1:1 HDT-DAT	88 ± 5	7.2 ± 0.6	24.4 ± 1.6	790 ± 20	102 ± 9
0.95:1:0.05 HDT-DAT-PETMP	56 ± 2	6.1 ± 0.2	11.5 ± 1.4	330 ± 30	26 ± 4
0.9:1:0.1 HDT-DAT-PETMP	45 ± 5	5.3 ± 0.3	9.9 ± 2.1	280 ± 70	19 ± 7
0.95:1:0.05 HDT-DAT-TMPTMP	59 ± 2	6.1 ± 0.3	16.4 ± 1.3	510 ± 50	49 ± 4
0.9:1:0.1 HDT-DAT-TMPTMP	44 ± 4	5.1 ± 0.2	12.2 ± 1.0	370 ± 40	27 ± 4
1:0.95:0.05 HDT-DAT-TATATO	60 ± 2	6.5 ± 0.2	17.0 ± 0.3	500 ± 10	50 ± 2
1:0.9:0.1 HDT-DAT-TATATO	43 ± 2	4.7 ± 0.2	10.8 ± 2.4	350 ± 70	24 ± 8
1:0.95:0.05 HDT-DAT-TATM	54 ± 1	5.7 ± 0.2	21.7 ± 1.1	660 ± 60	68 ± 6
1:0.9:0.1 HDT-DAT-TATM	39 ± 2	4.1 ± 0.2	13.9 ± 0.7	460 ± 20	33 ± 3
1:0.95:0.05 HDT-DAT-TABT	63 ± 3	6.3 ± 0.2	24.5 ± 1.7	700 ± 10	86 ± 5
1:0.9:0.1 HDT-DAT-TABT	45 ± 3	5.1 ± 0.2	18.2 ± 1.0	580 ± 40	54 ± 7
1:0.95:0.05 HDT-DAT-TAT	73 ± 4	7.6 ± 0.4	23.4 ± 1.1	660 ± 30	84 ± 8
1:0.9:0.1 HDT-DAT-TAT	62 ± 7	6.5 ± 0.3	17.6 ± 0.9	520 ± 30	52 ± 5
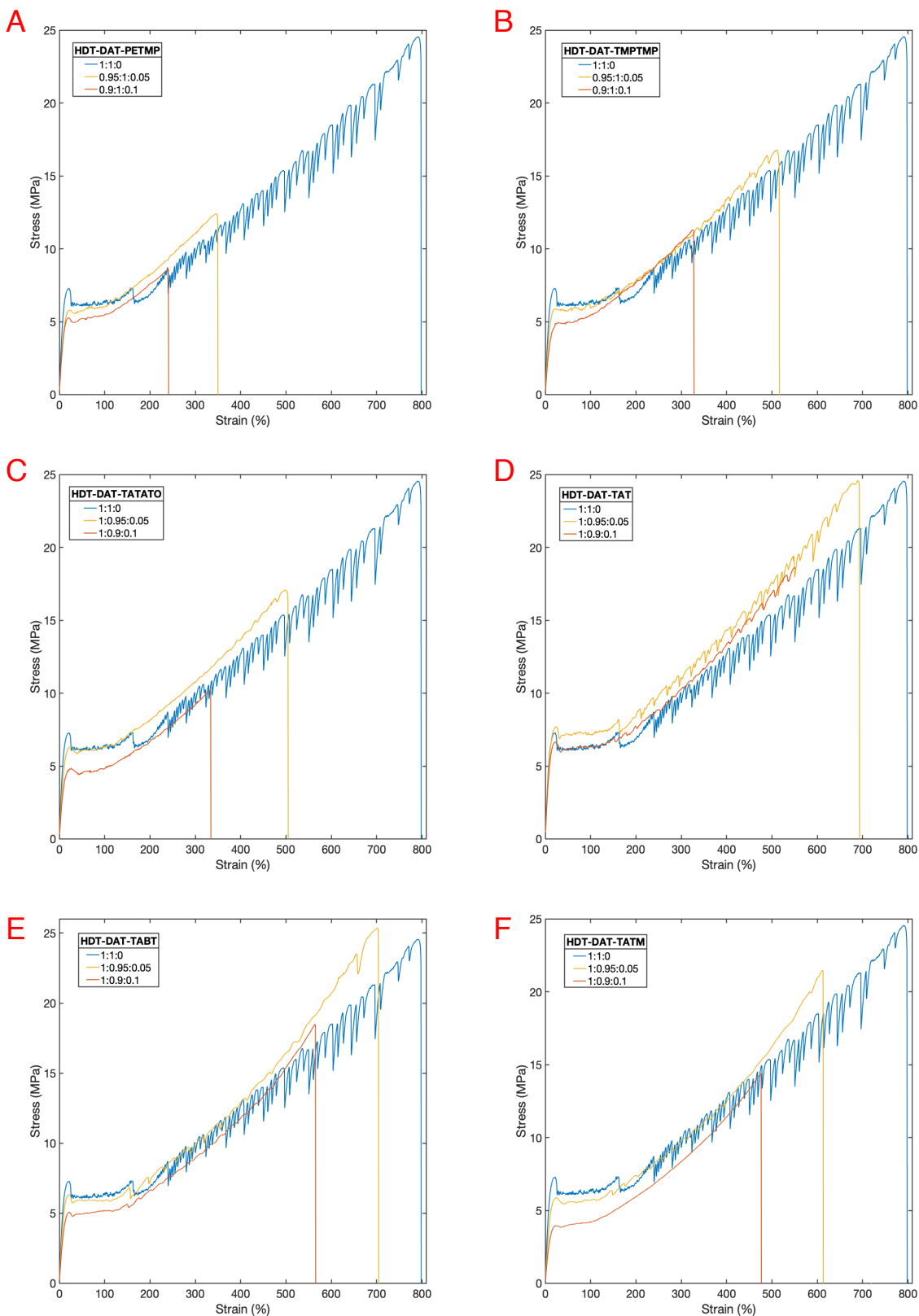
Fig. S1 Representative stress-strain plots of bulk thiol-ene formulations with varying amounts of cross-linker. ASTM D638 Type V dogbones were cut from a bulk film approximately 500 μm thick (prepared between glass slides and irradiated with a UV bar for 10 minutes on each side) and uniaxially strained at 5 mm min^{-1}.

Fig. S2 Dogbones with varying amounts of the crosslinker TAT were elongated to break. During plastic deformation, striations appeared on the dogbone that coincided with dips in the stress-strain profile. Striation appearance decreased with increasing crosslinking density and was in agreement with the decreasing frequency and intensity of the stress dips observed on the stress-strain profile.
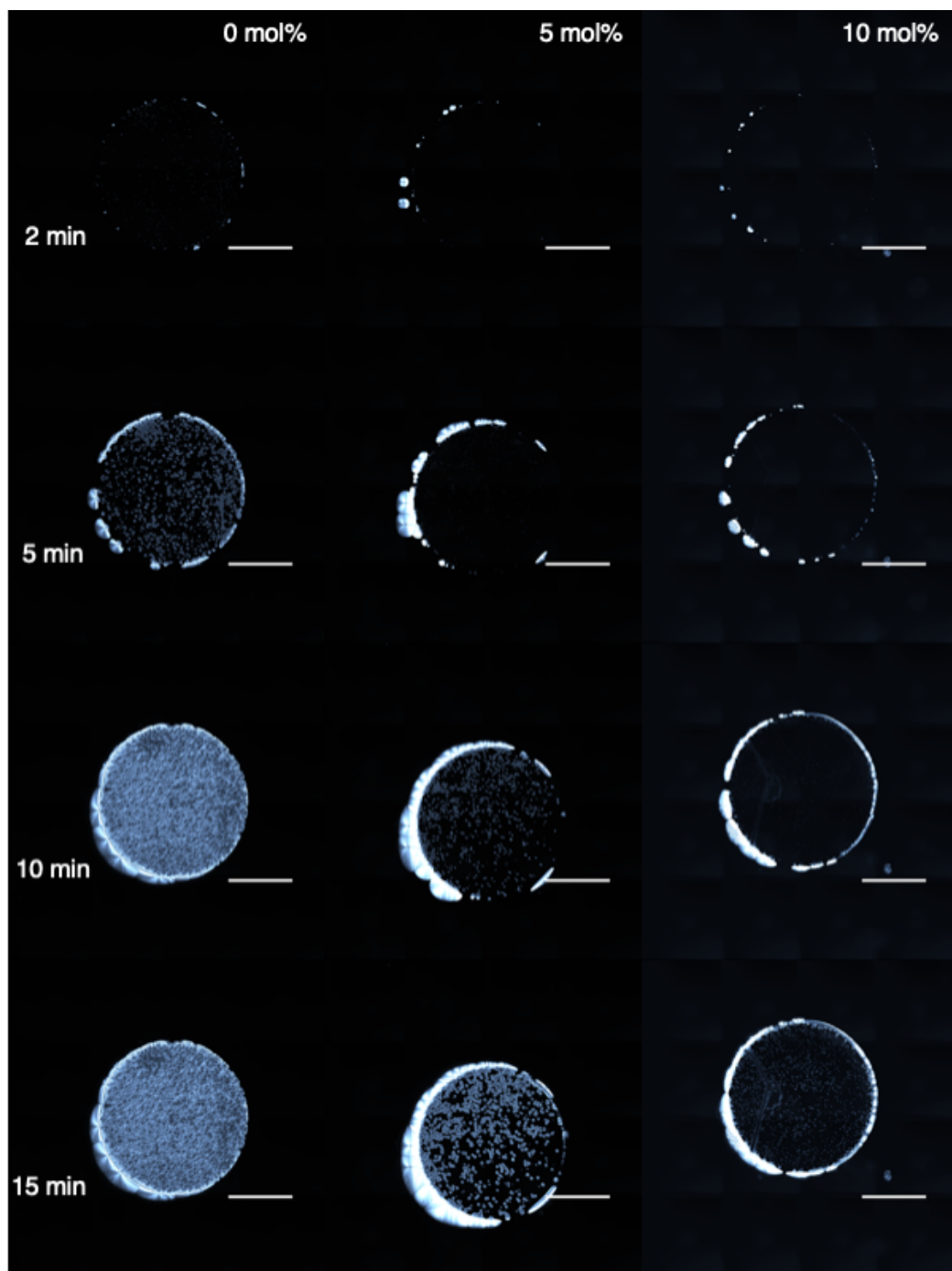
Fig. S3 Crystallization videos were obtained for samples containing 0, 5, and 10 mol% TAT. Samples were irradiated for 1 s, and videos were taken for each sample post-irradiation using a 20x objective. Crystallization occurred most quickly with decreasing cross-linker content, concurrent with that observed with photo-rheology.

Fig. S4 3D printed objects made with 1:0.9:0.1 (10 mol%) HDT-DAT-TAT: trophy (23.4 mm tall, 1.5 mm thick ears); solitaire ring setting (28.6 mm tall, 1.6 mm thickness ring support); bunny ring (20.4 mm ring size, 12.5 mm ear height); original Prusa SL1 test object (37 mm person height, 2 mm small hexagon size); lattice (27.3 mm width, 40.0 mm length, 25.0 mm height, 3.3 mm support thickness).
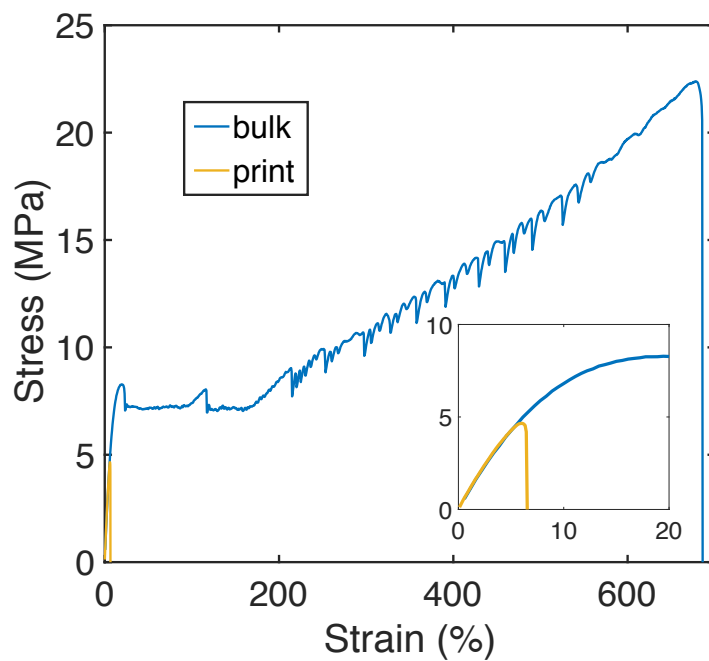
Fig. S5 Uniaxial tensile stress-strain plot of ASTM D638 Type V bulk and printed dogbones of 1:1 HDT-DAT strained at 5 mm min^{-1}. While the bulk material exhibited impressive ductility, the printed dogbone was brittle and fractured almost immediately.

Table S2 Mechanical properties obtained for the cross-linked and annealed prints. different cross-linkers at different concentrations. Printed ASTM D638 Type V dogbones were uniaxially strained at 5 mm min^{-1}. Failure stress is omitted for some samples as failure occurred shortly after yield. Annealing improved the mechanical properties of the cross-linked prints, while no improvement was observed for 1:1 HDT-DAT.

Sample	Thermal Conditioning (2 hours)	E (MPa)	Yield Stress (MPa)	Ultimate Tensile Stress (MPa)	Elongation at break (%)	Toughness (MJ m^{-3})
1:1 HDT-DAT	None	86 ± 11	3.7 ± 0.4	3.7 ± 0.4	4 ± 1	0.3 ± 0.2
1:1 HDT-DAT	70 °C	110 ± 3	3.4 ± 0.3	3.4 ± 0.3	3 ± 1	0.1 ± 0.05
1:1 HDT-DAT	80 °C	113 ± 4	2.7 ± 0.7	2.7 ± 0.7	2 ± 1	0.04 ± 0.02
1:0.95:0.05 HDT-DAT-TAT	None	64 ± 4	7.4 ± 1.9	7.4 ± 1.9	36 ± 21	2 ± 1.2
1:0.95:0.05 HDT-DAT-TAT	100 °C	69 ± 2	9.3 ± 0.4	10.2 ± 1.1	276 ± 68	17 ± 1
1:0.95:0.05 HDT-DAT-TAT	150 °C	64 ± 3	9.0 ± 0.2	15.9 ± 0.8	532 ± 33	59 ± 5
1:0.9:0.1 HDT-DAT-TAT	None	57 ± 1	8.2 ± 0.2	8.2 ± 0.2	50 ± 4	3.0 ± 0.4
1:0.9:0.1 HDT-DAT-TAT	100 °C	50 ± 1	7.3 ± 0.2	9.8 ± 1.2	226 ± 43	17 ± 5
1:0.9:0.1 HDT-DAT-TAT	150 °C	52 ± 1	7.5 ± 0.2	12.3 ± 0.6	362 ± 31	31 ± 3
1:0.9:0.1 HDT-DAT-TAT	200 °C	54 ± 2	7.3 ± 0.2	19.8 ± 0.3	787 ± 7	95 ± 1

Fig. S6 Printed 10 mol% TAT ASTM D638 Type V dogbone unconditioned and after thermal conditioning at 200 °C for 2 hours. No significant changes in print structure were observed upon heating at these temperatures.

Experimental

Materials
BAPO (Omnirad 819, formerly Irgacure®819) was gifted from IGM Resins USA, Inc. HDT (1,6-hexanedithiol, ≥ 97%), TAT (2,4,6-triallyloxy-1,3,5-triazine, 97%), PETMP (pentaerythritol tetrakis(3-mercaptopropionate), > 95%), TMPTMP (trimethylolpropane tris(3-mercaptopropionate), 95%), and TABT (triallyl 1,3,5-benzenetricarboxylate, 98%) were purchased from Sigma-Aldrich Co. DAT (diallyl terephthatlate, > 98%) was purchased from Tokyo Chemical Industry Co., LTD. Acetylene carbon black (CB) (100% compressed) was purchased from Strem Chemicals, Inc. TATATO (triallyl-s-triazine-2,4,6(1H,3H,5H)trione, 98%) was purchased from Acros Organics. TATM (triallyl trimellitate, 95%) was purchased from Combi-Blocks. All chemicals were used as received without further purification.

Methods

Bulk Photopolymer Film Preparation
Stoichiometric HDT-DAT and samples with 2, 5, and 10 mol% crosslinker relative to the corresponding thiol or ene substituent were mixed with 1 wt% BAPO. Films were deposited between large glass plates spaced with 500 μm rubber shims (high-temperature silicone rubber sheet, 50A, McMaster-Carr) and clamped together with binder clips. Films were irradiated for 5 minutes on each side with a 405 nm LED source (ECO UV Bar) at an intensity of approximately 7 mW/cm^2.

3D Printing
Stoichiometric thiol-ene printing formulations were prepared at 1:1 HDT-DAT, 1:0.95:0.05 HDT-DAT-TAT, and 1:0.9:0.1 HDT-DAT-TAT with 0.1 wt% carbon black, 1 wt% BAPO and 1 wt% of a proprietary additive to reduce surface tension donated by Colorado Photopolymer Solutions. A commercial LCD-based DLP printer (Prusa SL1) was used to print 1.6 mm thick dog bones (ASTM D368 Type V) at 50 μm layers with a burn time of 30 s and a layer exposure time of 15 s. All formulations were post cured with the 405 nm UV Bar after manufacture.

Annealing
Manufactured dog bones were annealed after printing and post cure irradiation. Samples were annealed for 2 hours at various temperatures in a benchtop Type 1300 Furnace (Barnstead/Thermolyne) at temperatures ≥ 100 °C and in a Model 10 Lab Oven (Quincy Lab Inc.) at temperatures < 100 °C.

Mechanical tensile testing
Uniaxial tensile tests (Exceed Model E42, 500 N load cell, MTS Systems Corporation) were performed on both bulk and printed samples. Samples were strained at a rate of 5 mm/min at ambient temperature. Young's modulus (E) was calculated from 1-5% strain from the linear elastic regime of the stress strain curve.

Shore Hardness
Shore D hardness was determined with a Phase II Digital Shore D Durometer. Hardness measurements of the printed material were performed in triplicate.

FTIR
A Nicolet 6700 FTIR spectrometer (Nicolet Magna-IR Series II, Thermo Scientific) with a MCT/A detector and a XT-KBr extended range beam splitter was used to monitor the conversion of both the thiol and carbon-carbon double bonds in real-time. Due to rapid polymerization rates, a temporal resolution of 1 scan/4 s was used with an optical velocity of 1.8988 cm/s, an optical gain of 1, and an optical aperture of 32. Samples were loaded between salt plates (International Crystal Laboratories) spaced with 50 μm plastic shims (Precision Brand). After 30 seconds, samples were irradiated with a collimated (SM2F32-A,

ThorLabs, Inc.) 405 nm LED (M405L4, ThorLabs, Inc.) at 1 mW/cm^2 for 10 seconds. Irradiation intensity was verified with a radiometer (PM100D Compact Power and Energy Meter Console, ThorLabs, Inc.). Thiol (2630.5-2483.4 cm^{-1}) and vinyl (1659.5-1635.4 cm^{-1}) peak area data were collected in real time using a series scan in OMNIC software (Thermo Scientific). Functional group conversion was determined as

$$Conversion = \left(1 - \frac{A_{final}}{A_{initial}}\right) * 100\% \tag{1}$$

where $A_{initial}$ is the peak area of the unreacted functional group, and A_{final} is the peak area of the consumed thiol or vinyl functional group after irradiation.

Photo-rheometer
Storage modulus (G'), loss modulus (G"), and complex viscosity (η*) were determined upon irradiation in real time using a rotational rheometer (ARES-G2, TA Instruments). A photocuring setup was implemented with a parallel plate geometry and a 20 mm diameter quartz plate for in-situ irradiation. After isothermally equilibrating at 25 °C for 1 minute, samples were irradiated with a collimated 405 nm LED (ThorLabs) after another minute at 25 mW/cm^2 for 10 seconds. The oscillation fast sampling procedure was used for 3600 s with a sampling rate of 4pts/s, a strain of 2%, and a frequency of 10 Hz. 68 μL of sample was pipetted between the plates and set to a gap of 0.2 mm.

POM
High resolution and temporal imaging were performed using a Nikon Ti-E microscope. Static images were obtained with 40x 0.95 NA objective. Crystallization videos were obtained using 20x 0.75 NA objective, and irradiation was performed for 1 s with an Excelitas Xcite 120 light source and a 360/40 nm excitation band pass filter. 4x4 images were obtained post-irradiation every 20 s for several minutes, and images and videos were analyzed with Nikon Elements software version 4.5.

DSC
Differential scanning calorimetry (DSC) was performed with a DSC2500 (TA Instruments) and was used to monitor thermal transitions. Approximately 6-7 mg of material was loaded into hermetically sealed aluminum pans (TA Instruments). To remain consistent with the crystallization conditions used while printing, materials were tested "as received", i.e. thermal history was not removed via an initial heating ramp.[1] Degree of crystallinity (% crystallinity) was calculated as

$$\% \ Crystallinity = \frac{\Delta H_m - \Delta H_c}{\Delta H_m^\circ} \tag{2}$$

where the heat of melting (ΔH_m) and the heat of cold crystallization (ΔH_c) are determined by integrating the areas under the peaks. ΔH_m° is a term that represents the heat of melting of a 100% crystalline material. Because no such value exists for the materials studied here, degrees of crystallinity were normalized to the heat of enthalpy for 1:1 HDT-DAT. Samples were equilibrated at -20 °C and ramped at 10 °C/min to 120 °C .

TGA
Thermal thiol-ene network stability for printed samples at each crosslinking density was measured with a thermogravimetric analyzer (PerkinElmer Pyris 1 TGA). All samples were heated from 20 °C to 850 °C at 10 °C/min under continuous nitrogen flow.